**Synthesis of defined oligohyaluronates-decorated liposomes and interaction with lung cancer cells**

# Synthesis of defined oligohyaluronates-decorated liposomes and interaction with lung cancer cells

Maria Emilia Cano [a], David Lesur [a], Valeria Bincoletto [b], Elena Gazzano [c], Barbara Stella [b], Chiara Riganti [c], Silvia Arpicco [b,*], José Kovensky [a,*]

[a] *Laboratoire de Glycochimie, des Antimicrobiens et des Agroressources CNRS UMR 7378, Université de Picardie Jules Verne, 33 rue Saint Leu, 80039 Amiens, France*

[b] *Department of Drug Science and Technology, University of Torino, Via Giuria 9, 10125 Torino, Italy*

[c] *Department of Oncology, University of Torino, Via Santena 5/bis, 10126 Torino, Italy*

*Corresponding authors: silvia.arpicco@unito.it; jose.kovensky@u-picardie.fr

Hyaluronic acid (HA) oligosaccharides of degree of polymerization (DP) 4, 6 and 8 were obtained by enzymatic depolymerization of HA. After chemical modification, these oligosaccharides were conjugated to a PEG-phospholipid moiety and the products (HA-DP4, HA-DP6 and HA-DP8) were used to prepare decorated liposomes. Liposomes displayed a dimensional range of about 160 nm and a negative charge that slightly increased as the conjugate molecular weight increased confirming the presence of glycoconjugates on their surface. The cellular uptake of HA-DP4, HA-DP6 and HA-DP8-decorated fluorescently labelled liposomes was significantly higher in lung cancer cell lines with high CD44 expression (A549, NCI-H1650) than in those with low CD44 expression (NCI-H1385, NCI-H228), suggesting a receptor-mediated entry of HA-conjugated formulations. HA-DP4, HA-DP6 and HA-DP8-liposomes did not show cytotoxicity or inflammatory effects, opening the perspective of their employment in nanomedicine.

Keywords: Hyaluronic acid; oligosaccharides; liposomes; HA-CD44 interaction

## 1. Introduction

Hyaluronic acid (HA) is a widely distributed extracellular matrix polysaccharide of the glycosaminoglycan family. It is a polymer of high molecular weight composed of alternating glucuronic acid and *N*-acetylglucosamine units forming a repeating sequence of the disaccharide β-D-GlcA-(1→3)-β-D-GlcNAc-(1→4). This biomolecule is involved in the regulation of inflammation, tumor development and healing processes through its interaction with different proteins (Fuster & Esko, 2005; Toole, 2004).

HA is considered as a key biomarker of specific cancers, because CD44, the main receptor of HA at the cell surface, is overexpressed on different solid (colon, ovarian, breast, lung) tumors and leukemias. The binding of HA to CD44 modulates the regulation and the proliferation of cancer cells. Recently, it has been reported that the repeating sequence of HA provides multiple binding sites for CD44 binding, inducing CD44 clustering, an event related to tumor progression and inflammation processes (Yang et al., 2012).

This binding has prompted researchers to use HA-phospholipid conjugates to construct liposomes able to target tumor cells through the CD44 receptor. In previous works, it has been shown that such liposomes can successfully bind to cells, and if they are loaded with anticancer drugs as gemcitabine or doxorubicin derivatives, they can be internalized and delivered efficiently. (Arpicco et al., 2013; Dalla Pozza et al., 2013; Gazzano et al., 2019; Marengo et al., 2019).

Like other polymers, macromolecular HA is not homogeneous: indeed, it is composed of multiple chains of different length, with an average molecular weight of about $10^6$ Da. Oligosaccharides of lower molecular weight that can be obtained by chemical or enzymatic depolymerization, also bind CD44. However, it has been reported that a mixture of oligosaccharides with a degree of polymerization (DP) 4-20 exhibits pro-inflammatory effects, while HA polysaccharide exerts opposite effects (Gao, Yang, Mo, Liu, & He, 2008). This difference has been interpreted in terms of monovalent vs. multivalent interactions. Clustering of CD44 would require multivalent HA-CD44 binding

occurring with the HA polymer, whereas HA oligosaccharides could only allow monovalent interactions, thus preventing the receptor clustering. (Yang et al., 2012)

In this paper, we explore the use of small HA oligosaccharides of defined structure and purity. Our approach involved the chemical modification of these oligosaccharides (DP4, 6 and 8) and conjugation to a phospholipid moiety. These conjugates were used to prepare liposomes, which present at the surface a multivalent arrangement of these small oligosaccharides. After complete characterization of the liposomes, the cellular uptake by human lung cancer cells, the cell viability and the inflammatory profile were studied.

## 2. Materials and methods

### *2.1. Materials*

Fetal bovine serum (FBS), fluorescein-5-(and-6)-sulfonic acid trisodium salts and culture medium were from Invitrogen Life Technologies (Carlsbad, CA). Plasticware for cell cultures was from Falcon (Becton Dickinson, Franklin Lakes, NJ). All the phospholipids were provided by Avanti Polar-Lipids distributed by Sigma-Chemical Co (St. Louis, MO). The protein content in cell extracts was assessed with the BCA kit from Sigma Chemical Co. Unless otherwise specified, all the other reagents were purchased from Sigma Chemical Co.

### *2.2. Enzymatic hydrolysis of hyaluronic acid*

Sodium hyaluronate (2 g) was dissolved in 0.1 M sodium acetate buffer (41 mL, pH 4.5) at 37 °C and bovine testes hyaluronidase (BTH, 12800 U) was added. After stirring for 2 days at 37 °C, 6000 U of enzyme were added. The addition of enzyme was repeated until TLC (n-butanol/formic acid/water, 2:2:1) showed no further changes (15 days). The solution was heated at 80°C for 5 min, filtered to remove the denatured enzyme, and freeze-dried. The crude product was desalted on Sephadex LH-20 using water as eluent. Analytical anion exchange chromatography (HPAEC) of the oligosaccharide mixture showed the presence of DP4, 6 and 8 as the main products.

78 *2.3. Purification of oligosaccharides of DP4, DP6 and DP8 of hyaluronic acid*

79 The separation of the oligosaccharides was performed on a HPLC Waters autopurification
80 system (Waters, France) equipped with a 1525 binary pump coupled to a 2998 PDA
81 detector (Waters, France), and a SEDEX LT-ELSD LC detector (Sedere, France). The run was
82 performed at room temperature, the compounds were loaded on a TSKgel DEAE 5PW
83 column (10 µm particle size, 200 mm x 50 mm) and the sample injection volume was 700
84 µl (aqueous solutions of compounds at 140 mg/mL). The mobile phase consisted of 1mM
85 ammonium formate (solvent A) and 1M ammonium formate (solvent B). The composition
86 of the mobile phase varied during the run as follows:

87 *Condition prep:* A:B: 0-20 min (100:0 to 85:15 v/v), 20-50 min (85:15 to 62:38 v/v), 50.01-
88 60 min (0:100 v/v) at a flow rate of 30 mL/min.

89 Data acquisition and processing were performed with MassLynx V4.1 software.

90 After lyophilization, compounds **1a**, **1b** and **1c** were obtained in pure form in 14%, 16%
91 and 17% yield, respectively.

92 *2.4. Direct azidation of the oligohyaluronans of DP4, 6 and 8*

93 Compounds **2a**-**c** were synthesized using a previously described methodology (Köhling et
94 al., 2019). Briefly, 2-chloro-1,3-dimethylimidazolinium (DMC, 118 mg, 0.7 mmol) was
95 added to a solution of oligohyaluronans (0.07 mmol), *N*-methylmorpholine (212 mg, 2.1
96 mmol) and $NaN_3$ (273 mg, 4.2 mmol) in water at 0 °C. The mixture was stirred at room
97 temperature for 30 h and then was evaporated under reduce pressure. The 1-
98 azidooligosaccharides **2a** and **2b** were purified on a Sephadex LH-20 column using
99 deionized water to give the pure tetra- and hexasaccharide derivatives in 68% and 65%
100 yield, respectively. The analytical data were in accordance to those previously reported
101 (Köhling et al., 2019, 2016). The octasaccharide derivative was desalted using a Cellulose
102 Ester (CE) dialysis membrane (MWCO: 100-500 Da) to afford **2c** (69 mg, 63% yield). $^1$H
103 NMR ($D_2O$, 400 MHz) $\delta$ 4.80 (1H), 4.50-4.47 (m, 3H), 4.44-4.40 (m, 4H), 3.94-3.71 (m, 24H),

3.63-3.51 (m, 12H), 3.40-3.32 (m, 4H), 2.04 (s, 3H, Ac), 2.03 (2s, 9H, Ac); $^{13}$C NMR ($D_2O$, 101 MHz) $\delta$ 174.9 (*C*O), 103.0, 102.9, 100.7 (C-1), 88.5 (C-1 $N_3$), 82.9, 82.4, 81.9, 79.9, 77.4, 75.7, 75.5, 75.4, 75.3, 75.2, 73.6, 72.6, 72.3, 71.5, 68.4, 68.3, 60.5, 54.3, 54.2, 22.4; ESI-HRMS (positive ion): *m/z* [*M*+Na]$^+$ calcd for ($C_{56}H_{85}N_7O_{44}Na^+$): 1582.4527; found: 1582.4531.

*2.5. General procedure for click reaction*

DSPE-PEG(2000)-DBCO **3** (10 µmol) was dissolved in water (473 µL). An aqueous solution of the sugar residues (10 µmol in 190 µL of water) was added, the mixture was stirred at room temperature for 1 h and then was lyophilized. Compound **4a**: ESI-HRMS (neg.): *m/z* [*M*-2H]$^{3-}$ calcd. for ($C_{179}H_{316}N_8O_{78}P^{3-}$): 1285.6888; found: 1285.6915. Compound **4b**: ESI-HRMS (neg.): *m/z* [*M*-H]$^{2-}$ calcd. for ($C_{193}H_{338}N_9O_{89}P^{2-}$): 2118.5969; found: 2118.6045. Compound **4c**: ESI-HRMS (neg.): *m/z* [*M*-2H]$^{3-}$ calcd. for ($C_{207}H_{358}N_{10}O_{100}P^{3-}$): 1538.4325; found: 1538.4259.

*2.6. Liposomes preparation and characterization*

Liposomes were prepared by the thin lipid film hydration and extrusion method. Chloroform solution of 1,2-distearoyl-*sn*-glycero-3-phosphocholine (DSPC), cholesterol (CHOL) and 1,2-distearoyl-*sn*-glycero-phosphoethanolamine-N-[amino(polyethylene glycol)-2000] (mPEG2000-DSPE) in a molar ratio 75:20:2 was mixed and evaporated under reduce pressure to obtain a thin lipid film. The resulting lipid film was hydrated with a 20 mM 4-(2-hydroxyethyl)piperazine-1-ethanesulforic acid (HEPES) buffer (pH 7.4) and vortexed for 10 min to obtain a suspension of multilamellar liposomes. The resulting suspension was then extruded (Extruder, Lipex, Vancouver, Canada) 10 times under nitrogen through 200 nm polycarbonate filter at 60°C.

To prepare decorated liposomes (LipoHA-DP4, LipoHA-DP6, LipoHA-DP8), the same method was used. Lipid films were made up of DSPC/CHOL/mPEG2000-DSPE (75:20:2

129 molar ratio) and then hydrated using solution of the different HA-DP conjugates **4a**, **4b**
130 and **4c** (3 molar ratio) in HEPES buffer.

131 Fluorescently labeled liposomes were prepared as described above by adding 10 mM
132 solution of fluorescein-5-(and-6)-sulfonic acid trisodium salts in HEPES buffer during the
133 hydration of the lipid film. The unentrapped fluorescein was removed by gel filtration
134 using Sepharose® CL-4B column eluting with HEPES buffer. Liposomes were stored at 4 °C.

135 The mean particle size and polydispersity index (PI) of the liposomes were determined at
136 25 °C by quasi-elastic light scattering (QELS) using a nanosizer (Nanosizer Nano Z, Malvern
137 Inst., Malvern, UK). The selected angle was 173° and the measurement was made after
138 dilution of the liposomes suspension in MilliQ® water. Each measure was performed in
139 triplicate.

140 The particle surface charge of liposomes was investigated by zeta potential measurements
141 at 25 °C applying the Smoluchowski equation and using the Nanosizer Nano Z.
142 Measurements were carried out in triplicate.

143 *2.7. Cell cultures*

144 Human epithelial lung cells BEAS-2B, human non-small cell lung cancer cells A549, NCI-
145 H1385, NCI-H1975, NCI-H1650, NCI-H228, Calu-3 were purchased from ATCC (Manassas,
146 VA). Cells were grown in RPMI-1640 medium, supplemented with 10% v/v FCS and 1%
147 penicillin-streptomycin, at 37 °C, 5% $CO_2$, in a humidified atmosphere.

148 *2.8. Flow cytometry*

149 $1\times10^6$ cells were rinsed and fixed with 2% w/v paraformaldehyde (PFA) for 2 min, washed
150 three times with PBS and stained with the anti-CD44 antibody (Abcam, Cambridge, UK) for
151 1 h on ice, followed by an AlexaFluor 488-conjugated secondary antibody (Millipore,
152 Burlington, MA) for 30 min. $1\times10^5$ cells were analyzed with EasyCyte Guava™ flow

153 cytometer (Millipore), equipped with the InCyte software (Millipore). Control experiments
154 included incubation with non-immune isotype antibody.

155 *2.9. Cellular uptake*

156 $1\times10^5$ cells were seeded into a 96-well black plate, let to adhere for 6 h and incubated at
157 different time points with the fluorescently labeled liposomes as indicated in the Results
158 section. Cells were washed twice with PBS and rinsed with 300 µl PBS. The intracellular
159 fluorescence, an index of liposome uptake, was measured using a Synergy HT Microplate
160 Reader (Bio-Tek Instruments, Winooski, VT), using λ excitation 460 nm and λ emission 530
161 nm. Cells were then detached with tryspin/EDTA, sonicated and used for the measure of
162 intracellular protein contents. Results were expressed as fluorescence units (FU)/mg
163 cellular proteins.

164 *2.10. Cell viability*

165 $1\times10^4$ were seeded into a 96-well white plate, let to adhere for 6 h and incubated for 72 h
166 with the liposomes as indicated in the Results section. Cell viability was measured by the
167 ATPlite Luminescence Assay System (PerkinElmer, Waltham, MA), as per manufacturer's
168 instructions. Results were analyzed by a Synergy HT Microplate Reader. The luminescence
169 units of the untreated cells were considered 100%; the luminescence units of the other
170 experimental conditions were expressed as percentage versus untreated cells.

171 *2.11. Cytokine measurement*

172 1 ml of cell culture supernatant was collected after 24 h treatment and probed with the
173 Human Inflammation Antibody Array – Membrane (Abcam), as per manufacturer's
174 instructions. Results were quantified by densitometry analysis of each dot blot, using
175 Image J software (www.imagej.nih.gov). The dot blot density of untreated cells was
176 considered 1; results of the treatment conditions were expressed as fold change (density
177 of dot blot for each experimental condition/density of dot blot in untreated cells for the
178 same cytokine).

179 *2.12. Statistical analysis*

180 All data in the text and figures are provided as means ± SD. The results were analyzed by a
181 one-way analysis of variance (ANOVA) and Tukey's test. $p < 0.05$ was considered
182 significant.

183 **3. Results and discussion**

184 *3.1. Enzymatic treatment of hyaluronate and purification of hyaluronic oligosaccharides*

185 Sodium hyaluronate (HA) was incubated with bovine testes hyaluronidase (BTH), an
186 enzyme known for degrading HA to oligosaccharides. As BTH does not accept
187 tetrasaccharides as substrates (Mahoney, Aplin, Calabro, Hascall, & Day, 2001) extensive
188 enzymatic hydrolysis lead to the DP4 as the main product. We managed the reaction
189 conditions in order to obtain a mixture of oligosaccharides.

190 A preparative HPAEC-ELSD was used to purify the oligosaccharides, using a DEAE-cellulose
191 column and a gradient of aqueous solution of ammonium formate from 1mM to 1M as
192 eluent. The main compounds of the mixture were eluted at 23.7 (DP4, **1a**), 28.6 (DP6, **1b**)
193 and 32.7 min (DP8, **1c**) (Figure S1). After lyophilization, they were obtained in 14%, 16%
194 and 17% yield, respectively. The identity of these oligosaccharides was confirmed by $^{1}H$
195 NMR and ESI-MS.

196 *3.2. Synthesis of the phospholipo-oligohyaluronates*

197 In order to study the impact of the length of the sugar residue in the liposomes, the
198 oligohyaluronans were modify to perform the synthesis of the amphiphilic compounds. As
199 shown in Scheme 1, a direct azidation of anomeric position was performed with 2-chloro-
200 1,3-dimethylimidazolinium (DMC), *N*-methylmorpholine and $NaN_3$ in water at 0 °C.
201 Compounds **2a**, **2b** and **2c** were obtained in 68%, 65% and 63% yield, respectively. $^{13}C$
202 NMR spectra of compounds **2a**, **2b** and **2c** showed the diagnostic signal at 88.5 ppm
203 corresponding to the C1-$N_3$ (Figure 1).

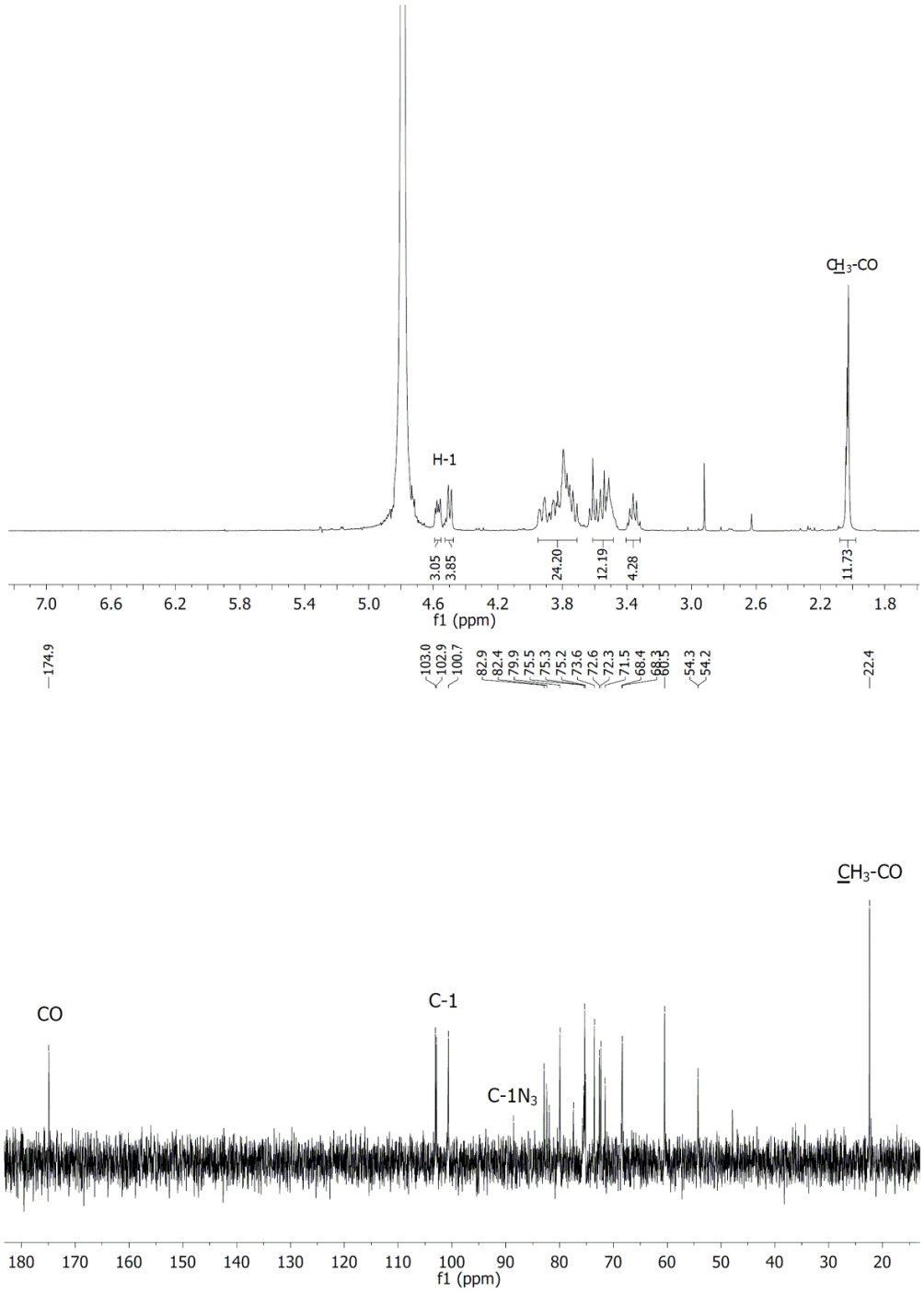


**Figure 1.** $^{1}H$ NMR (400 MHz) (top) and $^{13}C$ NMR (101 MHz) (bottom) spectra of compound **2c** recorded in $D_2O$ in a Bruker DRX 400.

207 Compounds **4a**, **4b** and **4c** were obtained by click reaction with DSPE-PEG(2000)-DBCO (**3**).
208 This azadibenzocyclooctyne reacted spontaneously with the corresponding
209 azidohyaluronate derivatives in water without addition of any catalyst, leading
210 quantitatively to phospholipo-oligosaccharides **4a**, **4b** and **4c**. These compounds were
211 characterized by ESI-HRMS. The spectra showed typical Gaussian profiles for the multi
212 charged ions with *m/z* values that correspond to the products.

213

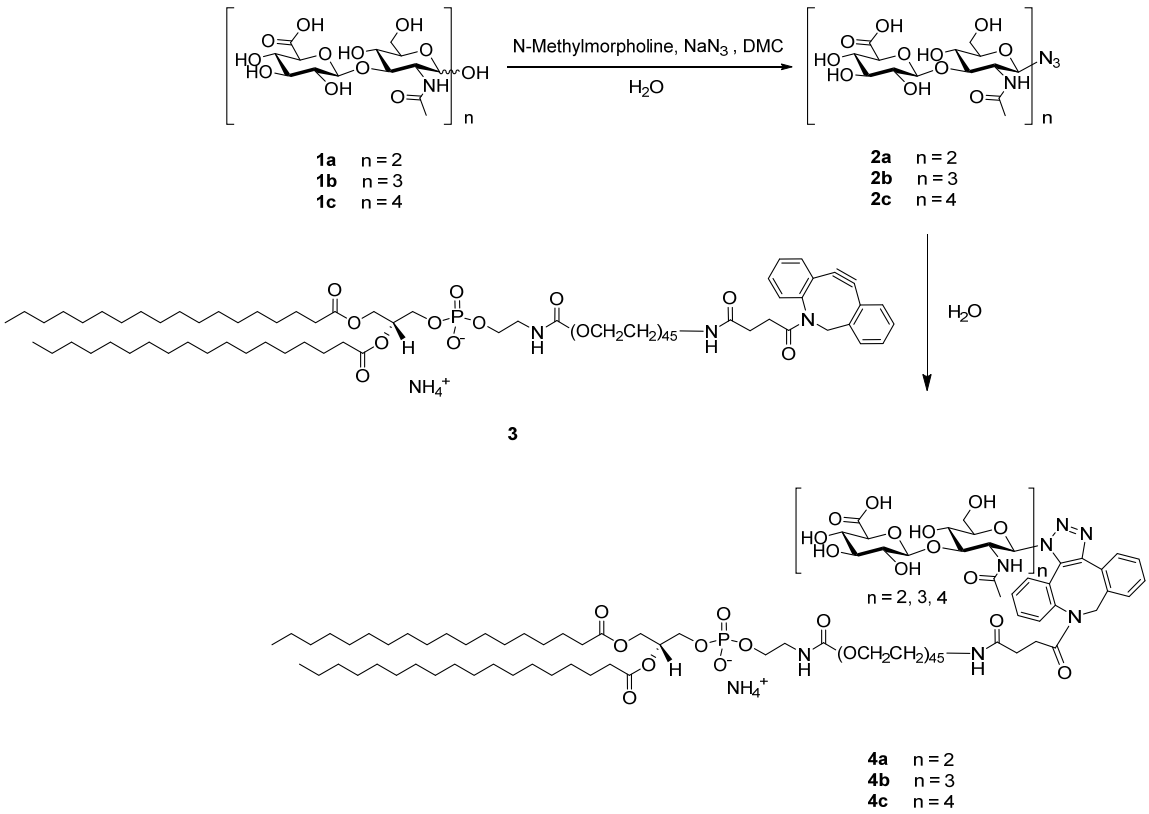


214

215 **Scheme 1.** Synthesis of phospholipo-oligohyaluronates.

216 *3.3. Preparation and characterization of liposomes*

217 Several papers report the preparation of HA decorated liposomes for the effective
218 delivery of drug to CD44-expressing cells (Dosio, Arpicco, Stella, & Fattal, 2016); basically,
219 two main approaches to insert HA into liposomes have been developed. In the first, HA is

220 linked to the surface of preformed liposomes by covalent conjugation between the
221 carboxylic residues of HA and phospholipid amine groups (Yerushalmi, Arad, & Margalit,
222 1994). This method offers the advantage to conjugate HA only on the external surface of
223 the particle but makes difficult the control the density of attachment of HA on the
224 liposomes. In the second method HA oligomers are previously conjugated to a lipid anchor
225 permitting the introduction of the conjugate into the lipid mixture during liposomes
226 preparation in a controlled amount (Arpicco et al., 2013; Eliaz & Szoka, 2001; Marengo et
227 al., 2019; Ruhela, Kivima, & Szoka, 2014).

228 To the best of our knowledge our compounds are the first examples of conjugates
229 composed of HA oligomers linked to PEG phospholipids. The presence of PEG should
230 improve the targeting ability of the systems decreasing the steric hindrance of the
231 liposomes in the ligand-receptor interaction.

232 The HA-DP4 (**4a**), HA-DP6 (**4b**) and HA-DP8 (**4c**) conjugates were added at a molar ratio of
233 3 during hydration to a lipid film composed of DSPC/CHOL/mPEG2000-DSPE (75:20:2
234 molar ratio). In this way, the phospholipidic chain was incorporated into the liposome
235 membrane, while the HA was exposed toward the aqueous phase; for comparison plain
236 liposomes were prepared without adding the conjugates. The physicochemical
237 characteristics of the different formulations are summarized in Table 1. Liposomes
238 displayed a dimensional range of about 160 nm and the polydispersity index was low for
239 all the formulations (< 0.18). Liposomes showed a negative Zeta potential value that was
240 lower for decorated liposomes compared to plain ones, due to the carboxylic negative
241 residues of conjugates. In particular, the negative charge slightly increased as the
242 conjugate MW increased confirming the presence of glycoconjugates on the surface of the
243 liposomes.

244 **Table 1**

245 Characteristics of plain and decorated liposomes. Values are the means ± SEM of three
246 independent experiments each performed in triplicate.

| Phospholipid composition | Mean particle size (nm) | Polydispersivity index | Zeta potential (mV) |
|---|---|---|---|
| **PLAIN**<br>DSPC/Chol/mPEG-DSPE 75:20:2 | 163 ± 1.3 | 0.115 | -9.3 ± 0.8 |
| **HA-DP4**<br>DSPC/Chol/mPEG-DSPE/**4a** 75:20:2:3 | 166 ± 1.5 | 0.175 | -27.1 ± 1.1 |
| **HA-DP6**<br>DSPC/Chol/mPEG-DSPE/**4b** 75:20:2:3 | 165 ± 1.8 | 0.166 | -32.6 ± 1.9 |
| **HA-DP8**<br>DSPC/Chol/mPEG-DSPE/**4c** 75:20:2:3 | 166 ± 1.6 | 0.149 | -35.3 ± 2.1 |

247

248 *3.4. Cellular uptake, viability and inflammatory profile*

249 We preliminary screened different human non-small cell lung cancer cell lines for their
250 expression of CD44, the receptor of HA, in comparison with non-transformed epithelial
251 lung cells BEAS-2B. While CD44 was poorly expressed in BEAS-2B cells, in the cancer cell
252 lines analyzed we detected cells with high (A549, NCI-H1650), moderate (NCI-H1975, Calu-
253 3) and low CD44 expression (NCI-H1385, NCI-H228) (Figure S2).

254 With the aim of understanding the significance of oligomer length for receptor binding,
255 we next evaluated the cellular uptake of the liposomes, by using fluorescently labelled
256 particles and measuring the intracellular accumulation of the fluorophore. All cell lines
257 displayed a dose-dependent uptake of the liposome cargo. In line with the different
258 expression of CD44, the uptake of HA-DP4, HA-DP6 and HA-DP8-decorated liposomes was
259 significantly higher in A549 and NCI-H1650 cells, and – to a lesser extent – in NCI-H1975
260 and Calu-3 cell, compared to plain liposomes. No differences in the uptake between
261 decorated and plain liposomes were detected in poorly expressing NCI-H1385 and NCI-
262 H228 cells (Figure 2). This experimental set suggests that the entry of HA-conjugated
263 formulations is likely receptor-mediated. Our hypothesis was confirmed by competition
264 assays performed on $CD44^{high}$ A549 and NCI-H1650 cells, incubated at different time
265 points with liposomes in the presence of a saturating amount of anti-CD44 antibody or
266 HA. As expected, the uptake increased over the time; such increase was higher with HA-

267 decorated liposomes than with plain liposomes. However, the presence of anti-CD44
268 antibody or HA blunted the uptake of HA-decorated liposomes (Figure 3).

269

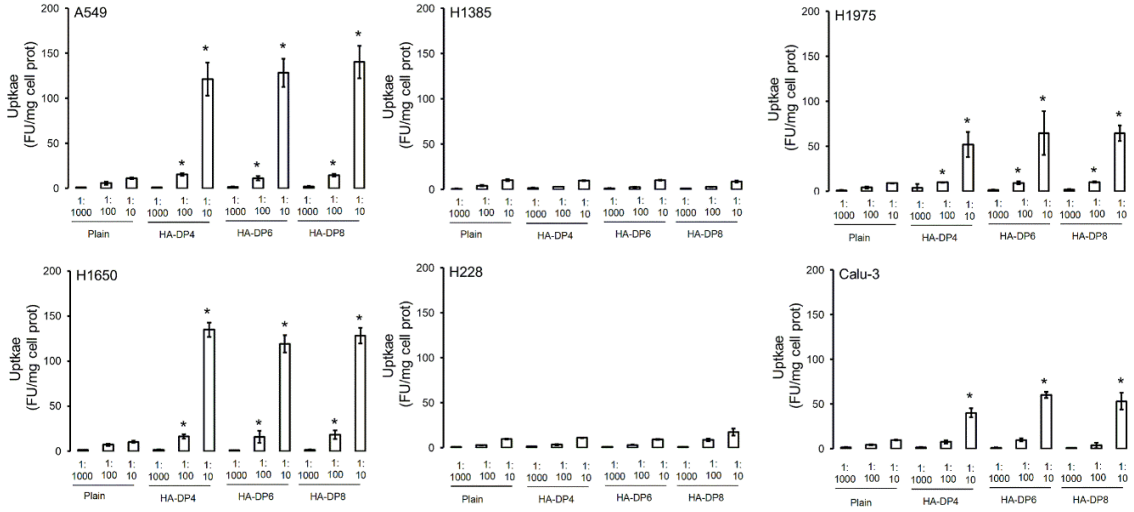


270

271 **Figure 2.** Cellular uptake of fluorescently labeled liposomes. A549, NCI-H1385, NCI-H1975,
272 NCI-H1650, NCI-H228, Calu-3 cells were incubated 24 h with fluorescently labelled plain
273 liposomes, HA-DP4-decorated, HA-DP6-decorated, HA-DP8-decorated liposomes, at a final
274 dilution in the culture medium of 1:10, 1:100, 1:1000. The intracellular content of
275 fluorescein, considered an index of liposome uptake, was measured
276 spectrofluorimetrically in triplicates. Data are means ± SD (n = 4). * $p < 0.05$: HA-
277 conjugated liposomes vs. corresponding plain liposomes.

278

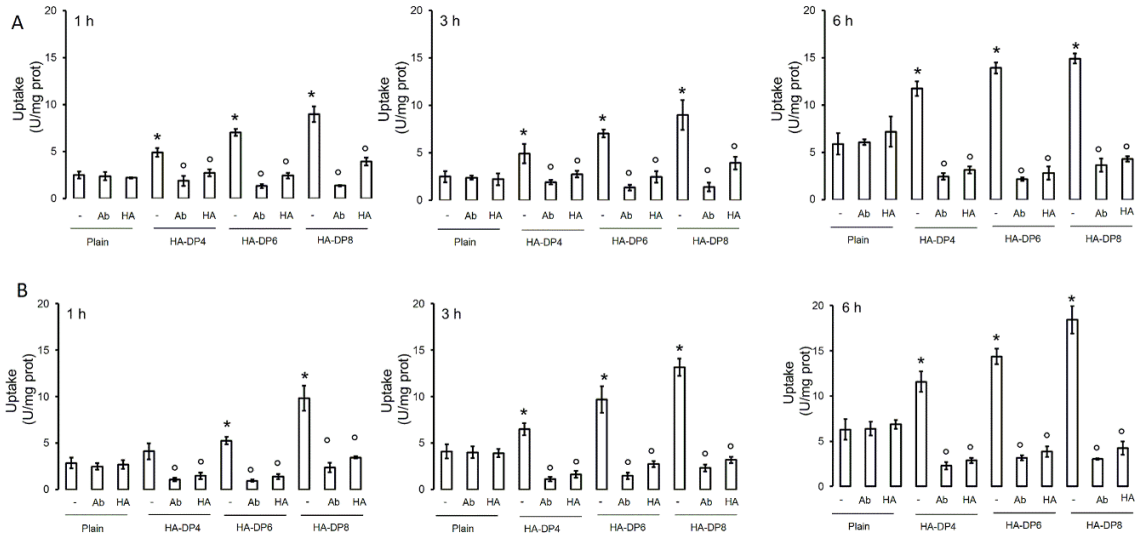


**Figure 3.** Competition assays in cellular uptake of fluorescently labeled liposomes. A549 (panel A) and NCI-H1650 (panel B) cells were incubated 1, 3 and 6 h with fluorescently labelled plain liposomes, HA-DP4-decorated, HA-DP6-decorated, HA-DP8-decorated liposomes, at a final dilution in the culture medium of 1:100, in the absence (-) or in the presence of an anti-CD44 antibody (Ab, at a final dilution of 1:10) or HA (100 µM). The intracellular content of fluorescein, considered an index of liposome uptake, was measured spectrofluorimetrically in triplicates. Data are means ± SD (n = 4). * $p < 0.05$: conjugated liposomes vs. corresponding plain liposomes; ° $p < 0.001$: Ab-HA-treated samples vs untreated (-) samples.

Interestingly, the amount of liposomes uptake at each time point followed this rank order: HA-DP8>HA-DP6>HA-DP4 liposomes at 1, 3 and 6 h (Figure 3), suggesting that the HA-DP8 formulations were optimal in inducing a fast receptor binding and triggering a receptor-mediated endocytosis.

To better compare the kinetics of entry of the liposomes with the structure of the conjugates used for their decoration, we analyzed the time-dependent uptake of liposomes prepared using conjugates previously synthetized in our laboratory (Arpicco et al., 2013) obtained by linking HA with two different molecular weight (4800 and 14800 Da)

297 to an aminated phospholipid by reductive amination. For this purpose, we used the highly
298 CD44-expressing A459 cells and the poorly CD44-expressing NCI-H228 cells. While in the
299 latter cell lines, there was always a lower uptake that did not change upon the time nor in
300 presence of an excess of HA, in A549 cells we observed that HA-4800 conjugates were
301 more taken up than HA-14800 conjugates at early time-points (1, 3 and 6 h). The
302 difference was not maintained at 24 h. After 3, 6 and 24 h, the uptake was drastically
303 reduced by HA in A549 cells, confirming that the intracellular delivery was CD44-
304 dependent (Figure S3).

305 This trend likely suggests that HA-DP4, 6 and 8 conjugates are capable of a faster
306 interaction with CD44, followed by phagocytosis, while the entry of the other HA-
307 conjugated liposomes requires more time. The sterical hindrance that makes the HA/CD44
308 interaction more complex and/or the need of CD44 clusterization upon the binding of
309 higher molecular weight HA conjugates may explain this difference. The presence of a PEG
310 chain between the phospholipid and the HA oligomer in our conjugates should also
311 improve the uptake. Moreover, at the same time point and in the same cell line, *i.e*. in the
312 presence of the same amount of CD44, the uptake of both 4,800-HA and 14,800-HA
313 conjugates was lower than the uptake of HA-DP4, the less effective conjugate in cellular
314 delivery (Figure 2, 3 and S3).

315 We finally analyzed the biocompatibility of our formulations. After 72 h incubation, either
316 unconjugated or HA-conjugated liposomes did not significantly reduce cell viability, in
317 both $CD44^{low}$ and $CD44^{high}$ cells (Figure S4). In parallel, none of the formulations changed
318 the expression of pro-inflammatory cytokines more than two-fold compared to untreated
319 cells (Figure S5). These two results suggest that in our experimental conditions the
320 liposomes are not cytotoxic and do not increase the release of potentially pro-
321 inflammatory mediators. DP4-20 have pro-inflammatory properties in biological systems
322 (Gao et al., 2008) and this side-effect may strongly limit the potential therapeutic
323 application of HA-conjugates. Our results suggest the safety – in terms of lack of

324 cytotoxicity and inflammatory effects – of HA-DP4, HA-DP6 and HA-DP8-liposomes,
325 opening the perspective of their employment in nanomedicine.

326 Indeed, exploiting the abundance of CD44 in non-small cell lung cancers (Chen, Zhao,
327 Karnad, & Freeman, 2018; Penno et al., 1994), HA decorated liposomes can be used for
328 the active targeting of anti-cancer drugs. Resistance to conventional chemotherapeutic
329 agents (Chang, 2011) or targeted-therapies used in specific patients subsets with
330 oncogenic mutations (Leonetti et al., 2018) is still a challenge in the therapeutic approach
331 of non-small cell lung cancers. The active targeting of tumors using anti-cancer drugs
332 encapsulated in liposomes is more effective that the administration of free drugs against
333 drug resistant tumors (Nag & Delehanty, 2019). This approach can improve in particular
334 the efficacy and pharmacokinetic profile of first-line drug in non-small cell lung cancers
335 such as cisplatin (Zhong et al., 2020). After evaluating the technical feasibility and binding
336 of our conjugates, we are next planning to load suitable anti-cancer drugs, deeply
337 characterize the formulations and evaluate their safety and anti-tumor efficacy against
338 CD44-expressing non-small cell lung cancers.

339 **4. Conclusions**

340 Novel conjugates between HA oligomers of different DP (4, 6 and 8) and PEGylated
341 phospholipid were prepared via click chemistry of 1-azido oligohyaluronates and
342 azadibenzocyclooctyne phospholipid. These conjugates were introduced during the
343 preparation of liposomes that were characterized in terms of size and zeta potential.

344 In order to evaluate their targeting *in vitro* studies on lung cancer cell lines with different
345 expression of CD44 were done, to assess the ability of cellular delivery and the lack of
346 toxicity or pro-inflammatory effects. This study is a proof of concept of the feasibility and
347 biocompatibility of HA-conjugates, and opens the way to their future development as
348 active-targeting agents carrying anti-tumor drugs.

349 **Supplementary material**

350 Purification of oligohyaluronates, surface expression of CD44 in lung cells, competition
351 assays in cellular uptake of HA-liposomes, viability and cytokine production from cells
352 treated with liposomes.

353 **Acknowledgments**

354 This work was supported by the Centre National de la Recherche Scientifique (CNRS),
355 l'Université de Picardie Jules Verne, the Agence Nationale de la Recherche (ANR-18-SUS2-
356 0001, France) and by the Italian Ministry for University and Research (MIUR)—University of
357 Torino, "Fondi Ricerca Locale (ex-60%)"

358 **References**

359 Arpicco, S., Lerda, C., Dalla Pozza, E., Costanzo, C., Tsapis, N., Stella, B., … Palmieri, M.
360 (2013). Hyaluronic acid-coated liposomes for active targeting of gemcitabine.
361 *European Journal of Pharmaceutics and Biopharmaceutics*, *85*(3 Part A), 373–380.
362 https://doi.org/10.1016/j.ejpb.2013.06.003

363 Chang, A. (2011). Lung Cancer Chemotherapy, chemoresistance and the changing
364 treatment landscape for NSCLC. *Lung Cancer*, *71*(1), 3–10.
365 https://doi.org/10.1016/j.lungcan.2010.08.022

366 Chen, C., Zhao, S., Karnad, A., & Freeman, J. W. (2018). The biology and role of CD44 in
367 cancer progression : therapeutic implications. *Journal of Hematology & Oncology*,
368 *11*(64), 1–23. https://doi.org/10.1186/s13045-018-0605-5

369 Dalla Pozza, E., Lerda, C., Costanzo, C., Donadelli, M., Dando, I., Zoratti, E., … Palmieri, M.
370 (2013). Targeting gemcitabine containing liposomes to CD44 expressing pancreatic
371 adenocarcinoma cells causes an increase in the antitumoral activity. *BBA -*
372 *Biomembranes*, *1828*(5), 1396–1404. https://doi.org/10.1016/j.bbamem.2013.01.020

373 Dosio, F., Arpicco, S., Stella, B., & Fattal, E. (2016). Hyaluronic acid for anticancer drug and
374 nucleic acid delivery. *Advanced Drug Delivery Reviews*, *97*, 204–236.
375 https://doi.org/10.1016/j.addr.2015.11.011

Eliaz, R. E., & Szoka, F. C. (2001). Liposome-encapsulated Doxorubicin Targeted to CD44 : A Strategy to Kill CD44-overexpressing Tumor Cells. *Cancer Research*, *61*, 2592–2601.

Fuster, M. M., & Esko, J. D. (2005). THE SWEET AND SOUR OF CANCER : GLYCANS AS NOVEL THERAPEUTIC TARGETS. *Nature Reviews Cancer*, *5*, 526–542. https://doi.org/10.1038/nrc1649

Gao, F., Yang, C. X., Mo, W., Liu, Y. W., & He, Y. Q. (2008). Hyaluronan oligosaccharides are potential stimulators to angiogenesis via RHAMM mediated signal pathway in wound healing. *Clinical and Investigative Medicine*, *31*(3), 106–116. https://doi.org/10.25011/cim.v31i3.3467

Gazzano, E., Buondonno, I., Marengo, A., Rolando, B., Chegaev, K., Kopecka, J., … Riganti, C. (2019). Hyaluronated liposomes containing H2S-releasing doxorubicin are effective against P-glycoprotein-positive / doxorubicin-resistant osteosarcoma cells and xenografts. *Cancer Letters*, *456*, 29–39. https://doi.org/10.1016/j.canlet.2019.04.029

Köhling, S., Blaszkiewicz, J., Ruiz-Gómez, G., Fernández-Bachiller, M. I., Lemmnitzer, K., Panitz, N., … Rademann, J. (2019). Syntheses of defined sulfated oligohyaluronans reveal structural effects, diversity and thermodynamics of GAG-protein binding. *Chemical Science*, *10*(3), 866–878. https://doi.org/10.1039/c8sc03649g

Köhling, S., Künze, G., Lemmnitzer, K., Bermudez, M., Wolber, G., Schiller, J., … Rademann, J. (2016). Chemoenzymatic Synthesis of Nonasulfated Tetrahyaluronan with a Paramagnetic Tag for Studying Its Complex with Interleukin-10. *Chemistry - A European Journal*, *22*(16), 5563–5574. https://doi.org/10.1002/chem.201504459

Leonetti, A., Assaraf, Y. G., Veltsista, D., El Hassouni, B., Tiseo, M., & Giovannetti, E. (2018). MicroRNAs as a drug resistance mechanism to targeted therapies in EGFR- mutated NSCLC: current implications and future directions. *Drug Resistance Updates*, *42*, 1–11. https://doi.org/10.1016/j.drup.2018.11.002

Mahoney, D. J., Aplin, R. T., Calabro, A., Hascall, V. C., & Day, A. J. (2001). Novel methods for the preparation and characterization of hyaluronan oligosaccharides of defined length. *Glycobiology*, *11*(12), 1025–1033. https://doi.org/10.1093/glycob/11.12.1025

Marengo, A., Forciniti, S., Dando, I., Dalla, E., Stella, B., Tsapis, N., … Palmieri, M. (2019). Pancreatic cancer stem cell proliferation is strongly inhibited by diethyldithiocarbamate- copper complex loaded into hyaluronic acid decorated liposomes Alessandro. *BBA - General Subjects*, *1863*(1), 61–72. https://doi.org/10.1016/j.bbagen.2018.09.018

Nag, O. K., & Delehanty, J. B. (2019). Active Cellular and Subcellular Targeting of Nanoparticles for Drug Delivery. *Pharmaceutics*, *11*(10), 543–570. https://doi.org/10.3390/pharmaceutics11100543

Penno, M. B., August, J. T., Baylin, S. B., Mabry, M., Linnoila, R. I., Lee, V. S., … Rosada, C. (1994). Expression of CD44 in Human Lung Tumors. *Cancer Research*, *54*, 1381–1388.

Ruhela, D., Kivima, S., & Szoka, F. C. (2014). Chemoenzymatic Synthesis of Oligohyaluronan − Lipid Conjugates. *Bioconjugate Chemistry*, *25*, 718–723. https://doi.org/10.1021/bc4005975

Toole, B. P. (2004). HYALURONAN : FROM EXTRACELLULAR GLUE TO PERICELLULAR CUE. *Nature Reviews Cancer*, *4*, 528–539. https://doi.org/10.1038/nrc1391

Yang, C., Cao, M., Liu, H., He, Y., Xu, J., Du, Y., … Gao, F. (2012). The High and Low Molecular Weight Forms of Hyaluronan Have Distinct Effects on CD44 Clustering * □. *The Journal of Biological Chemistry*, *287*(51), 43094–43107. https://doi.org/10.1074/jbc.M112.349209

Yerushalmi, N., Arad, A., & Margalit, R. (1994). Molecular and Cellular Studies of Hyaluronic Acid-Modified Liposomes as Bioadhesive Carriers for Topical Drug Delivery in Wound Healing. *Archives of Biochemistry and Biophysics*, *313*(2), 267–273. https://doi.org/10.1006/abbi.1994.1387

Zhong, Y., Jia, C., Zhang, X., Liao, X., Yang, B., Cong, Y., … Gao, C. (2020). European Journal of Medicinal Chemistry Targeting drug delivery system for platinum ( Ⅳ ) -Based antitumor complexes. *European Journal of Medicinal Chemistry*, *194*, 112229. https://doi.org/10.1016/j.ejmech.2020.112229